



## Direct Plating of Low Resistivity Bright Cu Film onto TiN Barrier Layer via Pd Activation

Jae Jeong Kim,<sup>\*z</sup> Soo-Kil Kim,<sup>\*</sup> and Yong Shik Kim<sup>\*</sup>

Research Center for Energy Conversion and Storage, School of Chemical Engineering,  
Seoul National University, Seoul 151-742, Korea

For seedless electroplating of low resistivity Cu film applicable to deep submicrometer damascene feature, Pd activation was introduced to direct Cu electroplating onto a high resistivity TiN barrier to get a high quality Cu film. Displacement-deposited Pd particles on the TiN substrate acted as nucleation sites for Cu plating. This high-density instantaneous nucleation made it possible to deposit a continuous, bright Cu film with low resistivity of 3.1  $\mu\Omega$  cm (after annealing). Aided by small amounts of benzotriazole, Pd activation also gave way to the application of seedless plating to superfilling of a deep submicrometer damascene structure, where the formation of the seed layer had been a critical issue. Poor adhesion between plated Cu and Pd activated TiN substrate was greatly improved by the addition of poly(ethylene glycol). The change in film characteristics was found to be negligible.

© 2003 The Electrochemical Society. [DOI: 10.1149/1.1633269] All rights reserved.

Manuscript submitted April 7, 2003; revised manuscript received July 7, 2003. This was Paper 699 presented at the Paris, France, Meeting of the Society, April 27-May 2, 2003. Available electronically December 9, 2003.

As feature size decreases to about 0.1  $\mu\text{m}$  according to the design rule, it is difficult to deposit a desirable Cu seed layer at the inside of trenches/vias owing to the inherent poor step coverage of physical vapor deposition (PVD). Therefore, electroless seed layer deposition methods or electrolytic seed repair methods were recently proposed as alternatives.<sup>1,2</sup> Although these methods could alleviate the difficulty in the seed layer preparation step, depositing Cu directly onto a diffusion barrier (e.g., TiN or TaN) without a seed layer would still be the most preferred process. Because of this, direct Cu electroplating onto the barrier material is emerging as a significant technological issue.

However, because almost all the barrier materials have higher electrical resistivities than Cu and have different crystal structures compared to Cu, direct Cu electroplating onto the diffusion barrier suffers from rough and discontinuous surface morphology caused by the coalescence of large clusters. To obtain a bright, continuous Cu deposited film, a large number of nuclei of small size is required. Previous research was mainly concerned about the Cu nucleation stage<sup>3-5</sup> to increase the density and reduce the size of the nucleus. Radisic *et al.*<sup>4</sup> reported that they obtained  $10^8$ - $10^{11}/\text{cm}^2$  Cu nucleus on a TiN barrier from pyrophosphate solution. Graham *et al.*<sup>5</sup> successfully filled a trench with ammonium sulfate solution. However, most of the previous research showed that nucleus sizes by direct plating was too large to fill deep submicrometer trenches/vias and that it was very difficult to get continuous, bright Cu film with low resistivity.

Accordingly, development of a new nucleation method that could provide a bright, low resistivity Cu deposit is the goal of this study. A HF-based Pd activation process that has been used in Cu electroless plating<sup>6</sup> was selected as a new nucleation step to give bright Cu film without a Cu seed layer. Near-10 nm Pd particles on the TiN layer might act as nuclei for Cu electroplating.

Though the Pd treatment to enhance the Cu nucleation in Cu metallorganic chemical vapor deposition (MOCVD) process was once proposed,<sup>7</sup> the replacement of the Cu seed layer with near-10 nm Pd nuclei in Cu electroplating is a novel process. This study investigated direct Cu electroplating on the TiN diffusion barrier using Pd activation as a substituted nucleation step. The possibility for applying this process at the deep submicrometer scale trenches was also demonstrated.

### Experimental

The substrates used in the experiments were (100) oriented p-type blanket and trench-type patterned (aspect ratio of 2.5) Si wafers coated with CVD TiN (10 nm) / PVD Ti (15 nm) as a diffusion barrier layer.

Prior to Pd activation, the TiN surface of the substrate was cleaned by 1% HF solution to remove a native Ti oxide formed on a TiN layer. Pd activation on this pretreated TiN layer was performed by dipping the wafer into an activating solution composed of PdCl<sub>2</sub> (0.28 mM), HCl (36.5 mM), and HF (185.2 mM)<sup>6,8</sup> for 40 s.

Cu electroplating onto blanket TiN layers both without and with Pd activation (denoted as substrate T and substrate P, respectively) was performed in the base electrolyte composed of 1 M H<sub>2</sub>SO<sub>4</sub>,

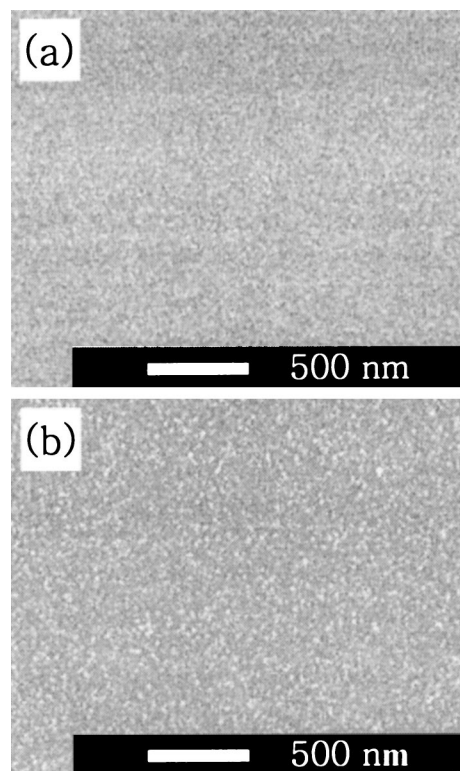
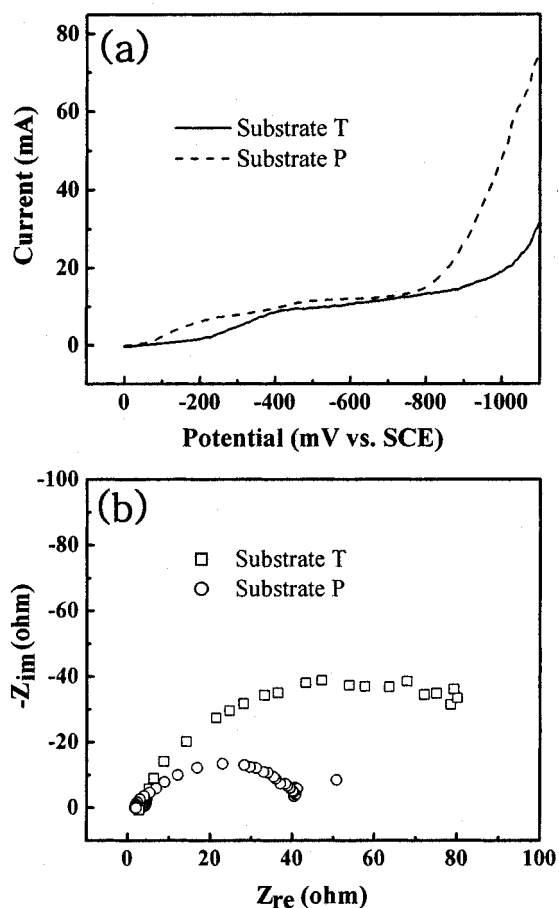


Figure 1. FESEM images of (a) substrate T (TiN without Pd activation) and (b) substrate P (Pd activated TiN).

\* Electrochemical Society Active Member.

<sup>z</sup> E-mail: jkimm@snu.ac.kr



**Figure 2.** (a) LSV and (b) EIA of Cu electroplating on each substrate. The sweep rate for LSV was 20 mV/s and EIA was performed at  $-500$  mV vs. SCE with 5 mV with the ac signal superimposed on it.

0.05 M  $\text{CuSO}_4 \cdot 5\text{H}_2\text{O}$ , and DI water. The effect of poly(ethylene glycol) (PEG, Mw 3400) as an adhesion promoter on the plating characteristics was examined by addition of 0.12 mM PEG in the base electrolyte. On the other hand, electroplating on patterned TiN substrate was carried out in two steps, electroplating on Pd-activated patterned TiN substrate in the base electrolyte with 0.12 mM PEG for 40 s as a seeding process, and further electroplating in the base electrolyte with 0.84 mM benzotriazole as a suppressor to

fill the structure<sup>9</sup> for 100 s. For electroplating on a patterned substrate, the Cu source concentration in the base electrolyte was increased up to 0.25 M to avoid Cu ion depletion inside the damascene structure. The first step was needed in gap filling since the function of benzotriazole strongly correlated with the interaction with the Cu surface.<sup>9</sup> Constant potentials for Cu electroplating ( $-500$  mV) were applied by an EG&G PAR 263 potentiostat (EG&G Princeton Applied Research Corporation) with respect to a saturated calomel electrode (SCE) at room temperature. A Cu bar was used as the anode for Cu electroplating. After electroplating, all samples were rinsed with DI water and dried in a  $\text{N}_2$  stream. Annealing at  $400^\circ\text{C}$  for 30 min in a  $\text{N}_2$  atmosphere<sup>9</sup> was done to further increase adhesion strength and make the electrical property better through grain growth. Commercial 3M brand scotch tape was used for the adhesion test.

Electrochemical impedance analysis (EIA) using an EG&G PAR 5210 lock-in amplifier (EG&G Princeton Applied Research Corporation) and linear sweep voltammetry (LSV) were conducted to investigate the plating phenomena on both T and P substrates. An ac signal with an amplitude of 5 mV and a frequency range between 100 kHz and 0.1 Hz was used in EIA. The scan rate for LSV was 20 mV/s. Field emission scanning electron microscopy (FESEM, Philips XL30FEG), four-point probe (Chang Min CMT-SR1000N), atomic force microscopy (AFM, Digital Instruments Dimension<sup>TM</sup> 3100), X-ray diffractometer (XRD, MAC Science M18XHF-SRA) measurement, and Auger electron spectroscopy (AES, Perkin-Elmer model 660) were applied to study the film properties of plated Cu on each substrate.

## Results and Discussion

Figure 1 presents the surface FESEM images of substrate T (TiN without Pd activation) and substrate P (Pd activated TiN). CVD TiN (Fig. 1a) shows a smooth, bright surface with a root mean square (rms) roughness of less than 1 nm. After dipping in the Pd activation solution, Ti atoms on the TiN surface were dissolved out by HF and then replaced with Pd particles marked as bright spots in the SEM image (Fig. 1b). The number density of Pd particles of substrate P was  $6.5 \times 10^{10}/\text{cm}^2$  with particle sizes of 10 to 20 nm. LSV of Cu electroplating on these substrates was performed with a base electrolyte, and the results are shown in Fig. 2a. The scan rate was 20 mV/s. At a given current, the electrode potential of substrate P was always smaller than that of substrate T. Therefore, the overpotential required to drive the plating reaction, which was the difference between the electrode potential and the equilibrium potential, was lower for electroplating on substrate P than for substrate T at the same temperature and  $\text{CuSO}_4$  concentration. Figure 2b exhibits the electrochemical impedance analysis of Cu electroplating on both substrates with a base electrolyte. The dc potential was  $-500$  mV

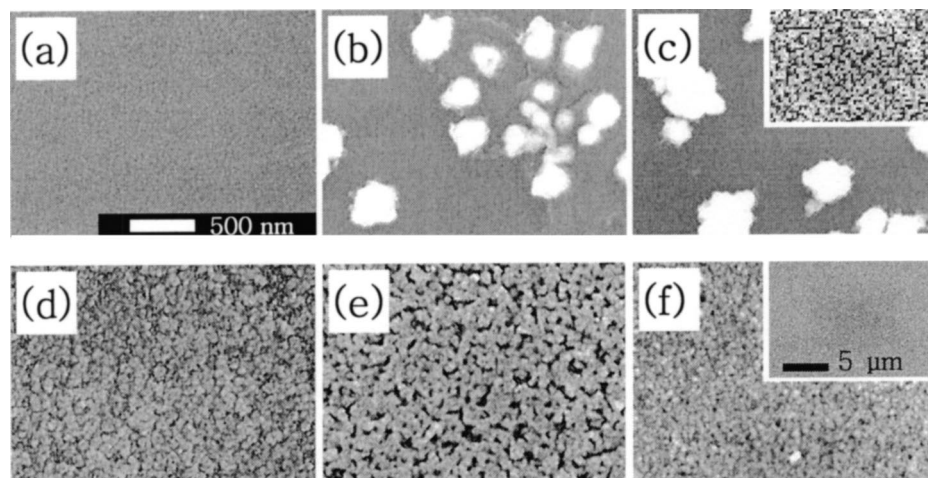


**Figure 3.** FESEM images of electroplated Cu on substrate T for (a) 1, (b) 5, and (c) 10 s and that on substrate P for (d) 1, (e) 5, and (f) 10 s. The small figures in (c) and (f) are electroplated Cu on substrate T and P for 2 min, respectively. Plating was performed in the base electrolyte at  $-500$  mV vs. SCE.

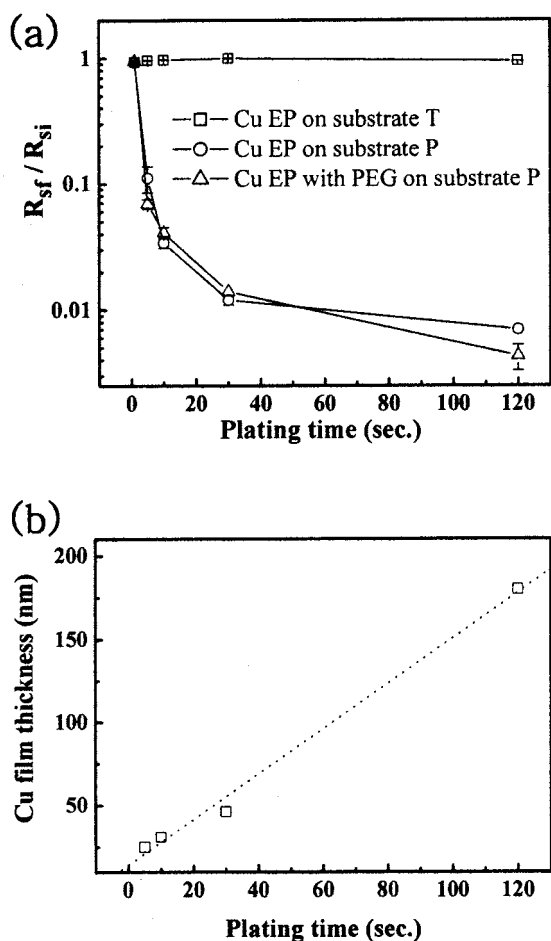


**Figure 4.** (a) Sheet resistance changes of electroplated Cu on both substrate T and P according to plating times and (b) thickness of Cu film on substrate P as a function of plating time.  $R_{si}$  and  $R_{sf}$  are the sheet resistances of the samples before and after Cu electroplating. Plating was performed in the base electrolyte at  $-500$  mV vs. SCE.

vs. SCE with 5 mV ac potential superimposed on it. As is clearly shown in the figure, the surface charge-transfer resistance for substrate P was smaller than that of substrate T, meaning Pd on substrate P served as a bridge for electron transfer through the interface between the TiN surface and the electrolyte. Consequently, Pd particles reduced the charge-transfer overpotential. The plating of Cu must preferentially take place at the Pd particles on the TiN substrate, exhibiting the role of Pd particles as nucleation sites.

An important observation in Fig. 2a is that substrate P suffered from faster hydrogen evolution (at about  $-870$  mV) than substrate T (at about  $-1040$  mV). This was because the minimum overpotential on the Pd surface needed for hydrogen evolution in an acidic medium was lower than most metals. Generated hydrogen causes a serious problem for the adhesion of plated Cu. This is discussed at a later section.

Plating behaviors of Cu on each substrate were observed using FESEM (Fig. 3). Plating was performed with a base electrolyte at  $-500$  mV. Figure 3a to c indicate 1, 5, and 10 s after Cu electroplating on substrate T while Fig. 3d to f represent those on substrate P. For Cu electroplating on substrate T, clusters were observed after several seconds of incubation time (less than 5 s). Further plating took place at the existing clusters by sticking to them, resulting in anisotropic growth (Fig. 3c). The number density of clusters did not increase with plating time, indicating that the plating on the TiN substrate followed instantaneous nucleation. Coalescence of clusters was observed after 2 min but the deposits still consisted of isolated

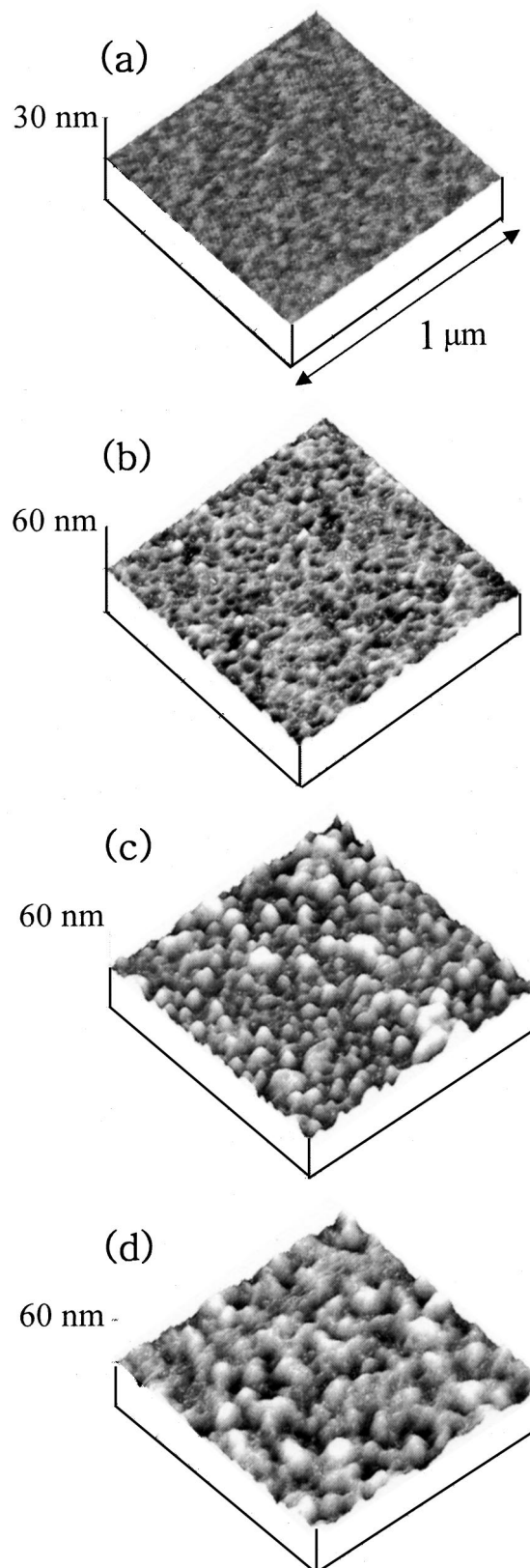


**Figure 5.** AFM images of (a) TiN surface after oxide etching, (b) TiN surface after Pd activation (substrate P), (c) plated Cu on (b) for 1 s, and (d) plated Cu on (b) for 5 s. The  $x$ - $y$  scale is  $1 \times 1 \mu\text{m}^2$  and  $z$  scale for (a) is 30 nm and that for (b) through (d) is 60 nm. Plating was performed in the base electrolyte at  $-500$  mV vs. SCE.

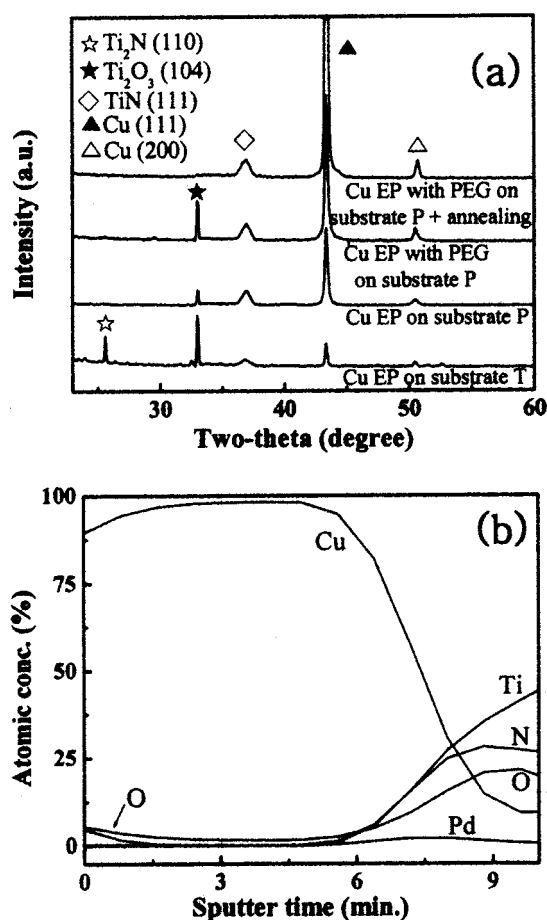


**Figure 6.** (a) XRD analysis of electroplated Cu films with different conditions and (b) AES depth profile analysis of electroplated Cu on substrate P. Plating was performed at  $-500$  mV vs. SCE.

clusters, not a continuous film. Accordingly, the sheet resistance of substrate T did not change with plating time, as shown in Fig. 4a.  $R_{si}$  and  $R_{sf}$  were the sheet resistances of the samples before and after Cu electroplating. The plated Cu clusters did not contribute to the reduction in the sheet resistance since the isolated clusters could not form a continuous path for the electric current. On the contrary, electroplating on substrate P showed a high number density of clusters even after 1 s of plating (Fig. 3d). Coalescence took place at 5 s (Fig. 3e) and a continuous film with a shiny surface was obtained after 10 s (Fig. 3f). Consequently, the sheet resistance of substrate P showed a sudden decrease with the progress of plating on account of the continuity of plated Cu film as presented in Fig. 4a. Figure 4b exhibits the relationship between plating time and the thickness of plated Cu film on substrate P. The linear fitted plating rate was about 82 nm/min, which is suitable to microelectronic fabrication.

Considering that the plating was preferentially proceeding at the Pd surface, plating on substrate P followed instantaneous nucleation with the role of Pd particle as a nucleation site. The number density of clusters depended on the number of Pd particles on the TiN surface. Based on Fig. 3, the number density of Pd particles of substrate P was about two times higher in order of magnitude than that of nucleation sites on substrate T. Therefore, Cu electroplating on Pd-activated TiN confirmed the high number density of instantaneous nucleation. This consideration was surveyed through AFM analysis (Fig. 5). Figure 5a to d represent the AFM images of oxide-etched TiN, substrate P, electroplated Cu on substrate P for 1 s, and that for 5 s, respectively. Compared with the bare TiN (Fig. 5a), displacement deposited Pd particles were observed as small protrusions on

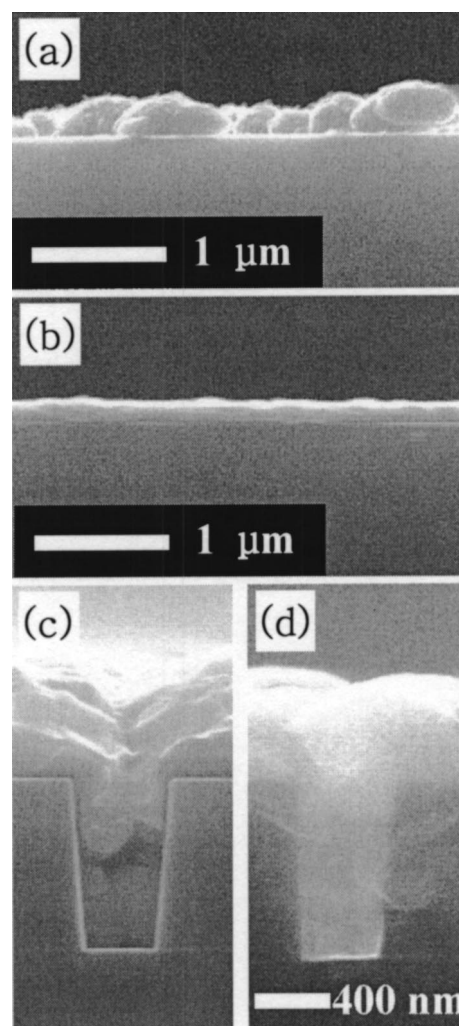


**Figure 7.** Cross-sectional FESEM images of electroplated Cu on (a) substrate T, (b) substrate P, (c) patterned substrate P with PEG, and (d) patterned substrate P at the presence of benzotriazole by two steps. (c) and (d) were performed with increased Cu source concentration (0.25 M  $\text{CuSO}_4 \cdot 5\text{H}_2\text{O}$ ) at  $-500$  mV vs. SCE.

the TiN surface (Fig. 5b). They provided nucleation sites for Cu plating (Fig. 5c). Growth and coalescence of clusters were also evident in Fig. 5d.

One important problem in the direct plating of Cu on the TiN substrate was poor adhesion between the TiN surface and the plated Cu layer. The main reason for this was the hydrogen evolution at the Pd surface during Cu electroplating, as previously mentioned. The adsorbed hydrogen with long residence time could disturb the adhesion strength of plated Cu. A solution for improving the adhesion strength is the addition of a surfactant such as PEG, which is known to remove the evolved hydrogen from the electrode surface in Cu electroless plating.<sup>10</sup> PEG at the presence of chloride ion ( $\text{Cl}^-$ ) is a well-known suppressor for superfilling of Cu electroplating.<sup>11-14</sup> However, from the sheet resistance measurement shown in Fig. 4a and from our previous investigation,<sup>15</sup> PEG in the absence of chloride ion had little effect on the plating characteristics.

As expected, the poor adhesion between Pd-activated TiN substrate and plated Cu was greatly improved with the addition of PEG and was strengthened enough to pass the adhesion test. Similar results regarding adhesion promotion using a PEG-like surfactant in Co electroplating was once reported.<sup>16</sup> Further improvement of adhesion strength was observed after 400°C annealing at nitrogen atmosphere. The annealing of substrate P prior to electroplating did not contribute to adhesion promotion.

Figure 6a exhibits the XRD analysis of plated Cu films. The preferred orientation of plated Cu film regardless of substrate was (111) and the small intensity of (200) peaks was also observed. However, a relatively weak (111) intensity of Cu film plated on substrate T compared to that on substrate P originated from the random or undeveloped texture of Cu film on substrate T. Removal of adsorbed hydrogen by the addition of PEG slightly enhanced the texture development of plated Cu on substrate P. Annealing at 400°C also contributed to the further increase in (111) intensity. The AES depth profile shown in Fig. 6b confirms the presence of the pure Cu film on substrate P with a trace amount of Pd at the interface between TiN and plated Cu.

Since the plated Cu on substrate T consisted of isolated clusters of different sizes (thickness) and did not form a continuous film as shown in Fig. 7a, there was little point in measuring the resistivity of plated Cu. In addition, the cluster size was near micrometer scale, which was too large to fill the submicrometer damascene features. However, Cu film plated on substrate P for 10 s, at which a continuous film can be formed, had a resistivity of 23.2  $\mu\Omega$  cm with a thickness of 30 nm. After a 30 s plating, the resistivity of about 50 nm thick Cu film decreased down to 4.43  $\mu\Omega$  cm. Further increase in plating time contributed to the reduction in the resistivity to a converged value of  $3.5 \pm 0.3 \mu\Omega$  cm. As an example, 180 nm thick Cu film on substrate P (Fig. 7b) was a continuous film with uniform thickness and low resistivity of 3.5  $\mu\Omega$  cm. After postdeposition annealing at 400°C for 30 min in nitrogen atmosphere, this resistivity was reduced to 3.1  $\mu\Omega$  cm. An attempt to fill the deep submicrometer damascene structure through Pd activation was made, and the results are shown in Fig. 7c and d. As shown in the Fig. 7c, direct plating on Pd-activated patterned TiN at the presence of PEG (as an adhesion promoter) showed discontinuous filling profile with voids at the middle of the trench. This was because the added PEG was not a suppressor since the electrolyte did not contain any chloride ions.<sup>15</sup> However, direct plating at the presence of benzotriazole (Fig. 7d) of which the detailed procedures were described in the Experimental section exhibited void-free filling in the trench. This result suggested the possibility of application of Pd activation to seedless direct plating on the high resistivity barrier layer to fill the deep submicrometer damascene structure.

### Conclusions

High quality continuous Cu film with well-developed texture and low resistivity was obtained by direct plating on Pd-activated TiN

substrate. Pd particles on the TiN surface served as high density nucleation sites that could replace a conductive Cu seed layer, which suggested a powerful solution for seedless Cu electroplating in deep submicrometer damascene structures. The addition of small amounts of PEG greatly improved the adhesion strength of the plated Cu film.

### Acknowledgments

This work was supported by KOSEF through the Research Center for Energy Conversion and Storage (RCECS), L. G. Chemical Limited, and also by the Institute of Chemical Processes (ICP).

Seoul National University assisted in meeting the publication costs of this article.

### References

1. J. J. Kim, S.-K. Kim, C. H. Lee, and Y. S. Kim, *J. Vac. Sci. Technol. B*, **21**, 33 (2003).
2. E. Webb, J. Sukamto, T. Andryushchenko, M. Danek, E. Klawuhn, R. Rozbicki, G. Alers, T. Suwwan de Felipee, V. Bhaskaran, A. Frank, K. Pfeifer, and J. Reid, in *Proceedings of the 18th VLSI Multilevel Interconnection Conference*, p. 42, Santa Clara, CA (2001).
3. G. Oskam, P. M. Vereecken, and P. C. Searson, *J. Electrochem. Soc.*, **146**, 1436 (1999).
4. A. Radisic, J. G. Long, P. M. Hoffmann, and P. C. Searson, *J. Electrochem. Soc.*, **148**, C41 (2001).
5. L. Graham, C. Steinbrüchel, and D. J. Duquette, *J. Electrochem. Soc.*, **149**, C390 (2002).
6. J. J. Kim and S. H. Cha, *Jpn. J. Appl. Phys., Part 1*, **40**, 7151 (2001).
7. J. Lim and C. Lee, *Solid-State Electron.*, **45**, 2083 (2001).
8. P. Bindra and J. Roldan, *J. Appl. Phys.*, **132**, 258 (1985).
9. J. J. Kim, S.-K. Kim, and J.-U. Bae, *Thin Solid Films*, **415**, 101 (2002).
10. Y. Shacham-Diamand, V. Dubin, and M. Angyal, *Thin Solid Films*, **262**, 93 (1995).
11. T. P. Moffat, J. E. Bonevich, W. H. Huber, A. Stanishevsky, D. R. Kelly, G. R. Stafford, and D. Josell, *J. Electrochem. Soc.*, **147**, 4524 (2000).
12. D. Josell, D. Wheeler, W. H. Huber, and T. P. Moffat, *Phys. Rev. Lett.*, **87**, 016102 (2001).
13. Y. Cao, P. Taephaisitphongse, R. Chalupa, and A. C. West, *J. Electrochem. Soc.*, **148**, C466 (2001).
14. A. C. West, S. Mayer, and J. Reid, *Electrochem. Solid-State Lett.*, **4**, C50 (2001).
15. Y. S. Kim, S.-K. Kim, and J. J. Kim, in *Proceedings of the 18th VLSI Multilevel Interconnection Conference*, p. 459, Santa Clara, CA (2001).
16. Y. Souche, J. P. Lévy, E. Wagner, A. Liénard, L. Alvarez-Prado, and R. T. Collins, *J. Magn. Magn. Mater.*, **242**, 578 (2002).